Wind Profile Estimation during Flight Path Reconstruction

T.K. Khadeeja Nusrath[*] and Jatinder Singh

CSIR-National Aerospace Laboratories, Bengaluru - 560 017, India
[*]*E-mail: khadeeja@nal.res.in*

ABSTRACT

Accuracy of flow angles measurements becomes crucial as the aircraft approaches higher angle of attack. Flight path reconstruction (FPR) is an excellent tool for air data calibration. An important element of air data calibration is the estimation of wind velocities. The objective of this paper is to evaluate different approaches of wind estimation within the framework of FPR. Flight test data of a high performance aircraft is subjected to FPR and the estimated wind velocities and flow angle trajectories are presented and discussed to demonstrate the impact of wind estimation on aircraft flow angles. Results clearly show that accuracy of reconstructed flow angles improves when time varying wind models are used. The proposed analytical wind model is found to be as effective as augmented parameters in Extended Kalman filter and computationally less intensive.

Keywords: Wind model; Flight path reconstruction; Flight data; Flow angles; Augmented state; State estimation; Extended Kalman filter

NOMENCLATURE

α	Angle of attack
β	Angle of sideslip
a_x, a_y, a_z	Acceleration in x, y, z axes
u, v, w	Inertial velocities in flight body axes
u_c, v_c, w_c	Body axes velocities corrected for wind
p, q, r	Aircraft angular rates
ϕ, θ, ψ	Aircraft Euler angles
ψ_a, γ_a	Wind axes Euler angles
V	True airspeed
h	Altitude
K_α, K_β	Scale factor in α and β
$\Delta\alpha, \Delta\beta$	Bias in α and β
$\Delta a_x, \Delta a_y, \Delta a_z$	Biases in accelerations
$\Delta p, \Delta q, \Delta r$	Biases in rates

1. INTRODUCTION

Flight path reconstruction[1] is a process used for evaluation of flight data quality before attempting aircraft system identification /parameter estimation. System identification has been the basis for extracting aerodynamic stability and control derivatives from aircraft flight test data[2]. These derivatives are useful not only to check for the deficiencies in the aero database derived from wind tunnel tests, but also in investigating the aircraft performance and aerodynamic characteristics, design of flight control laws and in conducting safe envelope expansion during prototype flight testing[3].

The success of system identification considerably depends on the quality of flight experiments and the recorded

data measurements. Several data inspection techniques are used by practicing engineers to check for the accuracy of the measurements. Initial checks are made by visual plots, examining the noise spectrum, slopes of the phase response and using redundancy in the measured variables. A more comprehensive approach is to use the complete 6DOF model for kinematic consistency checking[4-5].

The kinematic model for flight path reconstruction (FPR) used for data quality checks includes a set of first order differential equations that relate velocity components to linear accelerations and Euler angles to the body-fixed rotational rates. In FPR process, the inertial accelerations and angular rates are used as input variables and not as observations. Deterministic systematic instrumentation errors are modeled as scale factors, biases, and time shifts in the measured flight variables[6].

Flight path reconstruction procedure is an excellent tool for airdata calibration. Accurate measurements of flow angles are required not only for parameter estimation but are also vital for proper functioning of the flight control laws. Role of this exercise becomes more and more crucial as the aircraft approaches higher limits of angle of attack. An important element of airdata calibration is the estimation of wind velocities. The equations for FPR use inertial accelerations to compute the true airspeed components. This is strictly valid for the assumption of constant wind unless ground speed is used in the observation vector[7,8].

For computing true airspeed, angle of attack (AOA) and angle of sideslip (AOS), reliable estimation of wind components is necessary. If left unaddressed, this can become a dominant source of error. With highly improved instrumentation available today for data gathering, the sensor errors in biases and scale factors are likely to be small, thus leaving the wind

variations as the most possible reason for the inaccuracies in the reconstructed flight variables from FPR.

Several methods have been discussed in the literature to estimate wind velocity components from flight data. A popular approach is to use measurements from GPS and INS along with aircraft dynamic model to calculate the wind components[9-11]. Computing wind components from ATC data, especially for accident analysis, is discussed by Bach and Wingrove[12-13]. Brian[14] describes the process of air data calibration in full envelope from wind box manoeuvres. Results presented show limitation of time invariant wind formulations[15-16]. Application of time varying wind formulations as part of extended Kalman filtering to simulated data is demonstrated by Lee[17], *et al.*

The study presented in this paper is motivated by the need to evaluate the existing techniques for wind estimation under the stringent conditions of high AOA and altitude changes. The objective is to look for the approach that can provide the desired flow measurement accuracy and has ease of application to long duration manoeuvres. The aim is not to replace the existing approaches with a new one, but to decide which technique would yield better accuracy for a given flight condition and data measurements.

The most conventional approach is the constant wind model formulated within the framework of FPR. However, this technique poses several problems that limits its usefulness. It is shown in this paper that the constant wind model fails to yield accurate results for long duration manoeuvres, particularly when the variation in wind is large due to changes in altitude or heading[18]. The second approach is to use a time varying wind model to estimate the wind velocities from real flight test data of a manoeuvring aircraft. The estimation of unknown parameters in the error model is carried out using Extended Kalman Filter (EKF). EKF with stochastic modelling of wind components works well for long duration manoeuvres and yields wind estimates and air data flow angles with improved accuracy. However, improper tuning of the error covariance matrices may adversely affect the results from EKF[19]. Also, artificially defining wind components as additional states in EKF would increase the number of parameters in the error model, which may lead to observability and identifiability issues. Alternate approach is to use the analytical formulation, discussed in Ref.[12], for wind estimation. Application of this technique for wind estimation shows that it is equally effective and easier to use as part of FPR for obtaining true AOA and AOS from flight data. The flip side of this approach is that it mandatorily requires inertial velocity components and flow angle measurements whereas the state augmentation method (EKF) can yield results with reasonable accuracy even in the absence of inertial velocity component measurements.

2. FLIGHT PATH RECONSTRUCTION THROUGH STATE ESTIMATION

Flight path reconstruction (FPR) process combines kinematic model of the aircraft states with flight measurements to determine the true state trajectories along with the estimation of uncertainties in the sensor measurements such as scale factors, biases and time delays[4]. In the current investigations, FPR for the segmented as well as full flight data (take-off to

landing) is carried out using 9 states and 12 observations. The state vector includes the inertial velocity components in the body axis (u, v, w), the aircraft Euler angles(ϕ, θ, ψ), altitude h and positions (x, y). The model response is matched with the measurements from flight data. The flight data signals used in FPR analysis are the angle of attack α_m, side slip angle β_m, true air speed V_m, Euler angles (ϕ_m, θ_m, ψ_m) and pressure altitude h_m. Inertial (u_{gm}, v_{gm}, w_{gm}) velocities measured in NED frame and converted to body axis are also used in observation for improved estimation of the true velocity components u, v, w. GPS latitude and longitude are converted to x_{em}, y_{em} positions to compare with the estimated position of the aircraft in flight. The state model and observation model for FPR are given below[1].

State Model

$$\dot{u} = -(q - \Delta q)w + (r - \Delta r)v - g\sin\theta + (a_x - \Delta a_x)$$
$$\dot{v} = -(r - \Delta r)u + (p - \Delta p)w + g\cos\theta\sin\phi + (a_y - \Delta a_y)$$
$$\dot{w} = -(p - \Delta p)v + (q - \Delta q)u + g\cos\theta\cos\phi + (a_z - \Delta a_z)$$
$$\dot{\phi} = (p - \Delta p) + (q - \Delta q)\sin\phi\tan\theta + (r - \Delta r)\cos\phi\tan\theta$$
$$\dot{\theta} = (q - \Delta q)\cos\phi - (r - \Delta r)\sin\phi$$
$$\dot{\psi} = (q - \Delta q)\sin\phi\sec\theta + (r - \Delta r)\cos\phi\sec\theta$$
$$\dot{h} = u\sin\theta - v\cos\theta\sin\phi - w\cos\theta\cos\phi$$
$$\dot{x} = u\cos\psi\cos\theta + v(\sin\theta\cos\psi\sin\phi - \sin\psi\cos\phi)$$
$$\quad + w(\cos\psi\sin\theta\cos\phi + \sin\psi\sin\phi)$$
$$\dot{y} = u\sin\psi\cos\theta + v(\sin\psi\sin\theta\sin\phi + \cos\psi\cos\phi)$$
$$\quad + w(\sin\psi\sin\theta\cos\phi - \cos\phi\sin\phi) \tag{1}$$

where

$$u(0) = u_0, v(0) = v_0, w(0) = w_0, \phi(0) = \phi_0, \theta(0) = \theta_0,$$
$$\psi(0) = \psi_0, h(0) = h_0, x(0) = x_0, y(0) = y_0 \tag{2}$$

$\Delta a_x, \Delta a_y, \Delta a_z, \Delta p, \Delta q, \Delta r$ are the biases in linear accelerations and angular rates. To start with, initial values of the state variables are taken as the average of the first few values from the measurements and then iterated upon to get the correct estimates. Initial values of the biases are taken as zero.

Conversion of the inertial velocities in body axes obtained from Eqn. (1) to the earth-fixed reference frame (NED frame) is given by the transformation in Eqns. (3) and (4). Velocity vector from body to earth axis is transformed using the product of three rotation matrices L_{BE}.

$$\begin{bmatrix} u_g \\ v_g \\ w_g \end{bmatrix} = L_{BE} \begin{bmatrix} u \\ v \\ w \end{bmatrix} \tag{3}$$

$$L_{BE} = \begin{bmatrix} \cos\theta\cos\psi & \sin\phi\sin\theta\cos\psi - \cos\phi\sin\psi & \cos\phi\sin\theta\cos\psi + \sin\phi\sin\psi \\ \cos\theta\sin\psi & \sin\phi\sin\theta\sin\psi + \cos\phi\cos\psi & \cos\phi\sin\theta\sin\psi - \sin\phi\cos\psi \\ -\sin\theta & \sin\phi\cos\theta & \cos\phi\cos\theta \end{bmatrix}$$

$$L_{EB} = [L_{BE}]^T \tag{4}$$

After estimating W_x, W_y, W_z components of wind in body axis, the aircraft's the true airspeed V, flow angles α and β are

computed from the estimated states (u,v,w) using the relations given in Eqn. (5).

$$u_c = u - W_x$$
$$v_c = v - W_y$$
$$w_c = w - W_z$$
$$\alpha = \tan^{-1}(w_c / u_c)$$
$$\beta = \sin^{-1}(v_c / V)$$
$$V = \sqrt{(u_c)^2 + (v_c)^2 + (w_c)^2} \tag{5}$$

Details of the wind models to compute $W_x,$ W_y, W_z are given in Section 3.

Measurement Model

$$V_m = V$$
$$\alpha_m = K_\alpha \alpha + \Delta\alpha$$
$$\beta_m = K_\beta \beta + \Delta\beta$$
$$\phi_m = \phi$$
$$\theta_m = \theta$$
$$\psi_m = \psi \tag{6}$$
$$h_m = h$$
$$u_{gm} = u_g$$
$$v_{gm} = v_g$$
$$w_{gm} = w_g$$
$$x_{em} = x$$
$$y_{em} = y$$

In Eqn. (6), K_α and K_β denotes the calibration scale factors and $\Delta\alpha$ and $\Delta\beta$ are the unknown bias parameters which are estimated as part of a sensor model for α and β.

2.1 Flight Data Measurements

The linear accelerations a_X and a_Z to be used in Eqn.(1) are computed from the accelerometer measurements of a_{Xs} and a_{Zs}, by accounting for CG offset from sensor location, as given in Eqn. (7).

$$a_X = a_{Xs} + (q^2 + r^2)x_{scg} - (pq - \dot{r})y_{scg} - (pr + \dot{q})z_{scg}$$
$$a_Y = a_{Ys} - (pq + \dot{r})x_{scg} + (p^2 + r^2)y_{scg} - (qr - \dot{p})z_{scg}$$
$$a_Z = a_{Zs} - (pr - \dot{q})x_{scg} - (qr + \dot{p})y_{scg} + (p^2 + q^2)z_{scg} \tag{7}$$

where X_{scg}, Y_{scg}, and Z_{scg} represent the position of the accelerometers with respect to theCG.

The flight measurements used for matching the model observations include the attitude angles from INS, flow angles and true airspeed from air data sensors, and the inertial velocities and positions from GPS.

$$z = [V_m \ \alpha_m \ \beta_m \ j_m \ \theta_m \ \psi_m \ h_m$$
$$\qquad u_{gm} \ v_{gm} \ w_{gm} \ x_{em} \ y_{em}]^T \tag{8}$$

The state, input and the observation vectors for FPR are defined as

$$x = [\ u \ v \ w \ \phi \ \theta \ \psi \ h \ x \ y]^T$$
$$u = [a_x \ a_y \ a_z \ p \ q \ r]^T \tag{9}$$
$$y = [V \ \alpha \ \beta \ \phi \ \theta \ \psi \ h \ u_g \ v_g \ w_g \ x \ y \ ]^T$$

The unknown parameter vector to be estimated from flight data includes the wind velocity components and is given by

$$\Theta = [\Delta a_x, \Delta a_y, \Delta a_z, \Delta p, \Delta q, \Delta r, K_\alpha, \Delta\alpha,$$
$$K_\beta, \Delta\beta, W_n, W_e, W_d] \tag{10}$$

Estimation of the inertial wind velocity components W_n, W_e, W_d is discussed in the next section.

3. METHODOLOGY
3.1 Estimation Method

In the present study, FPR is carried out using Extended Kalman Filtering (EKF) technique. This is one of the most established approach for the aircraft state estimation in the presence of measurement as well as process noise. In EKF, by means of augmented state vector[3] given in Eqn. (11), parameter estimation is transformed into state estimation problem.

$$x_a = [x^T \Theta^T]^T \tag{11}$$

here the subscript a denotes the augmented state vector, where the additional parameters to be estimated are augmented to the state vector Θ. The state and observation models for a nonlinear system can be expressed for FPR as[1,3]

$$\dot{x}_a(t) = f\ [x_a(t), u(t)] + w(t)$$
$$y(t) = g\ [x_a(t), u(t)] \tag{12}$$
$$z(t_k) = y(t_k) + v(t_k)$$

where $w(t)$ and $v(t_k)$ are defined as Gaussian white state and measurement noise with zero mean and characterised with covariance matrices Q and R, respectively. $Z(t_k)$ represents the vector of observations at the kth time instant. The characteristics of the instrumentation used in the aircraft are used to define the measurement noise covariance matrix. The noise in the input signals (accelerations and rates) is considered as process noise[5]. Hence, the process noise covariance matrix is defined using the variances of the noise from accelerometer and rate gyro measurements. With flight data sampled at regular intervals, EKF uses the previous state estimate to predict the current estimate, thus providing solution for the mixed discrete/ continuous time causal system.

The two stages of the estimation using EKF are the prediction and correction steps as shown in Fig. 1. The prediction equations project forward (in time) the current state and the state error propagation covariance estimates to obtain the *a priori* estimates $\tilde{x}_k$ and $\tilde{P}_k$. In the correction step, *a posterior* estimate $\hat{x}_k$ and $\hat{P}_k$ are evaluated from the *a priori* estimates using the new measurements. More details on EKF can be obtained from references[2-4].

Prediction (extrapolation/time update)

$$\tilde{x}(k+1) = \hat{x}(k) + \int_{t_k}^{t_{k+1}} f[x(t), u(t_k), \Theta]\,dt$$

$$\tilde{P}(k+1) \approx \Phi(k+1)\hat{P}(k)\Phi^T(k+1) + \Delta t Q$$

where

$$\Phi(k+1) = e^{A(k)\Delta t} \approx I + A(k)\Delta t + A^2(k)\frac{\Delta t^2}{2!} + \dots$$

$$A(k) = \left.\frac{\partial f[x(t), u(t), \Theta]}{\partial x}\right|_{x=\hat{x}(k)}$$

Correction (measurement update)

$$\tilde{y}(k) = g[\tilde{x}(k), u(k), \Theta]$$

$$K(k) = \tilde{P}(k)C^T[C\tilde{P}(k)C^T + R(k)]^{-1}$$

$$\hat{x}(k) = \tilde{x}(k) + K(k)[z(k) - \tilde{y}(k)]$$

$$\hat{P}(k) = [I - K(k)C]\tilde{P}(k)[I - K(k)C]^T$$
$$\qquad + K(k)R(k)K^T(k)$$

where

$$C(k) = \left.\frac{\partial g[x(t), u(t), \Theta]}{\partial x}\right|_{x=\tilde{x}(k)}$$

Figure 1. EKF prediction and correction step.

3.2 Wind Velocities

Kinematics of the aircraft flying in the atmosphere disturbed by wind is defined by "wind triangle", as shown in Fig. 2(a). The wind-speed vector V_w is calculated by resolving the speed vectors V_a, the aircraft velocity relative to air, and the ground speed V_g. The true airspeed V (TAS) is determined by air data computer using the measurements from Pitot tube sensor[16]. V is then transformed to wind axis using wind axis Euler angles to obtain V_a as shown in Fig. 2(b). The ground speed V_g is measured by the inertial navigation unit and GPS. The wind vector is obtained by subtracting the air speed vector from the ground speed vector. The vector formulation to compute the wind speed is given by

$$\overline{V}_w = \overline{V}_g - \overline{V}_a \tag{13}$$

Flow chart for the 3 different approaches is given in Fig. 3. In approach 1 and 3, wind model is implemented in the state model and in approach 2, it is in the observation models. The mandatory and optional signals used in state and observation model for each case are stated.

Approach 1

The body axes velocities u, v, w from the state equation are contaminated with wind. Hence, the expression for positions x, y and h used in state model (Eqn. (1)) can be rewritten as given in Eqn. (14). Aircraft positions derived from GPS latitude and longitude are used as measurements to match the model observations as given in Eqn (6).

$$\begin{bmatrix} \dot{x} \\ \dot{y} \\ \dot{z} \end{bmatrix} = L_{BE}\begin{bmatrix} u_c \\ v_c \\ w_c \end{bmatrix} + \begin{bmatrix} W_n \\ W_e \\ W_d \end{bmatrix} \qquad \begin{matrix} x(0) = x_0 \\ y(0) = y_0 \\ z(0) = z_0 \end{matrix} \tag{14}$$

where

$$z = -h$$

Wind velocities computed in NED frame can be converted to body axis using the equation

$$\begin{bmatrix} W_x \\ W_y \\ W_z \end{bmatrix} = L_{EB}\begin{bmatrix} W_n \\ W_e \\ W_d \end{bmatrix} \tag{15}$$

where u_c, v_c, w_c are the corrected velocities in body axes during the previous time sample. Wind components in body axes W_x, W_y, W_z are obtained using transformation given in Eqn (15). In the present method, wind velocity components are treated as deterministic biases and, therefore, can be used only for manoeuvres where wind variation is minimal. Using this wind formulation, FPR can be implemented with other estimation techniques such as output error or filter error methods[6,14] which is the major advantage of this method.
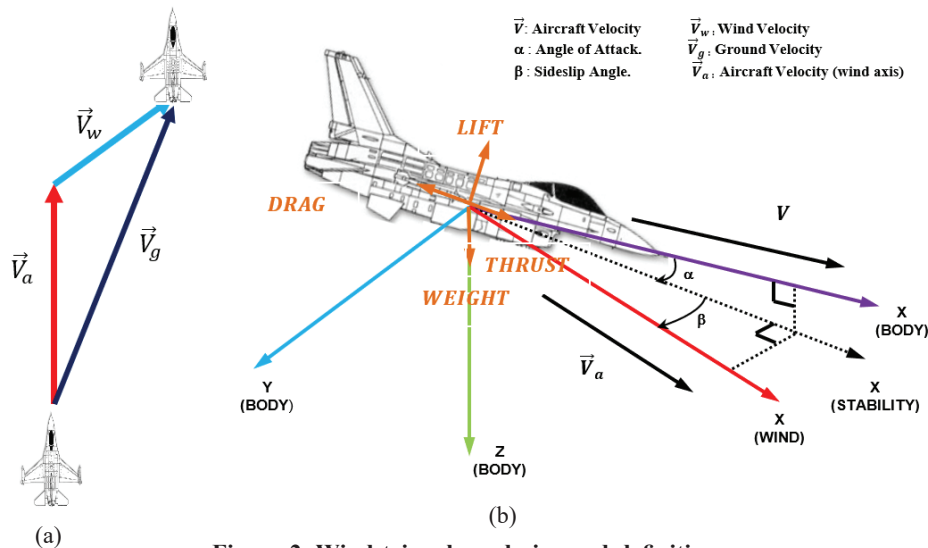

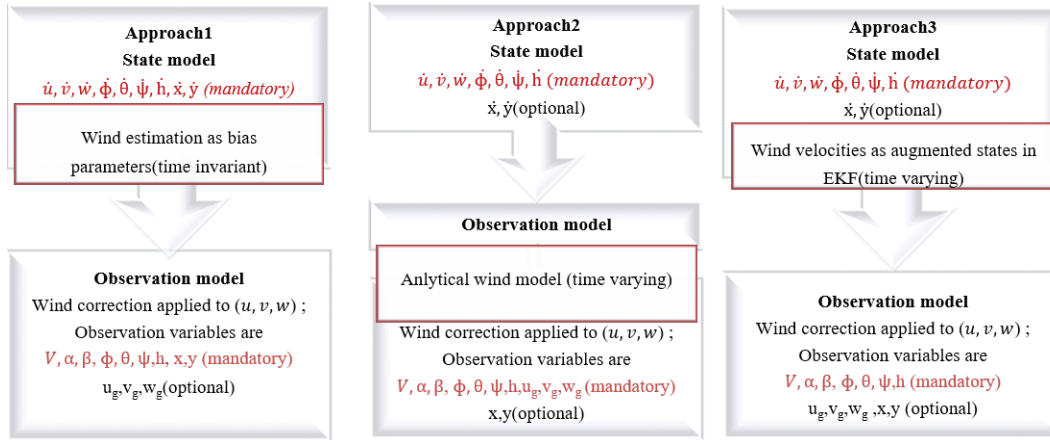**Figure 2. Wind triangle and airspeed definition.**

Figure 3. Flow chart for wind formulation.

Approach 2

In this approach, the wind triangle representation is used to compute the wind components from the true air speed and inertial velocities as shown in Eqns. (16) and (17). The inertial velocity components (u_g, v_g, w_g), the true airspeed measurement (V) from the pitot tube and wind axis Euler angles[12,20] are used in this formulation.

$$W_n = u_g - V\cos\psi_a\cos\gamma_a$$
$$W_e = v_g - V\sin\psi_a\cos\gamma_a \qquad (16)$$
$$W_d = w_g - V\sin\gamma_a$$

Where the wind axis Euler angles (γ_a, ψ_a) are calculated using the equations

$$\gamma_a = \sin^{-1}(\cos\alpha\cos\beta\sin\theta - C\cos\theta)$$
$$\psi_a = \tan^{-1}(\frac{\sin\beta\cos\phi - \sin\alpha\cos\beta\sin\phi}{\cos\alpha\cos\beta\cos\theta + C\sin\theta}) + \psi \qquad (17)$$
$$C = \sin\alpha\cos\beta\cos\phi + \sin\beta\sin\phi$$

This yields time varying wind which can be computed for full flight data. Parameters to be estimated are given in Eqn. (18), which are fewer when compared to Eqn. (10).

$$\Theta = [\Delta a_x, \Delta a_y, \Delta a_z, \Delta p, \Delta q, \Delta r, K_\alpha, \Delta\alpha, K_\beta, \Delta\beta] \qquad (18)$$

Since the wind components are not included in Θ, computational efficiency will be more with this formulation. However, this approach necessarily requires measurements of inertial velocity components for wind estimation.

Approach 3

In this approach, the wind components are treated as stochastic variables and are estimated as augmented states in the EKF.

$$\Theta = [\Delta a_x, \Delta a_y, \Delta a_z, \Delta p, \Delta q, \Delta r, K_\alpha, \Delta\alpha,$$
$$K_\beta, \Delta\beta, W_n, W_e, W_d] \qquad (19)$$

Since the wind is modelled as stochastic, it obviates the need to model the physical processes that govern wind behaviour. Note that the process noise covariance matrix Q is defined as nonzero for treating wind as stochastic and can be

tuned to improve the estimation accuracy[1,3]. Total wind and the wind direction can be calculated using the relation

$$W_{tot} = \sqrt{(W_x)^2 + (W_y)^2 + (W_z)^2}$$
$$W_{dir} = \tan^{-1}(W_y / W_x) \qquad (20)$$

4. RESULTS AND DISCUSSIONS

In this section, flight data analysis results from a high performance fighter aircraft in different flight regimes are used for illustration. Using the approaches discussed above, wind velocities are estimated and compared to demonstrate how different wind formulations affect the estimation of wind components, which in turn affects the accuracy of estimated flow angles.

4.1 Wind Velocity Components from Flight Data

Figures 4 to 6 show the results of wind estimation when flight path reconstruction is carried out for the data gathered during roller coaster and pitch doublet manoeuvre in windup turn. Table 1 lists the estimated bias values in accelerometers and rate gyros during FPR. The small values of standard deviation indicate accurate estimation of bias parameters.
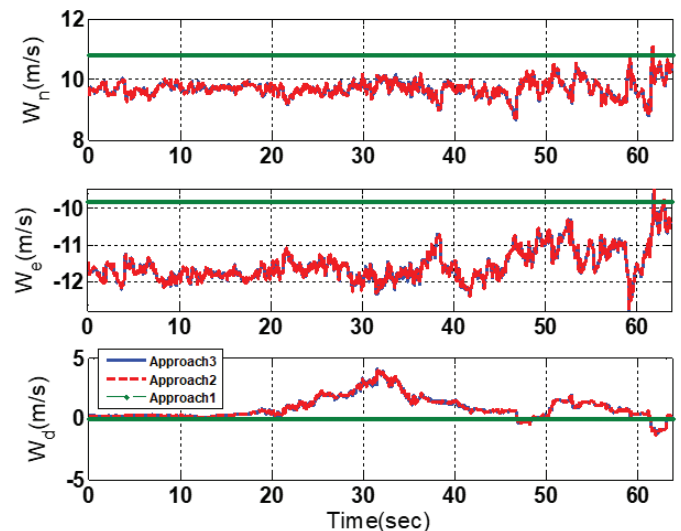

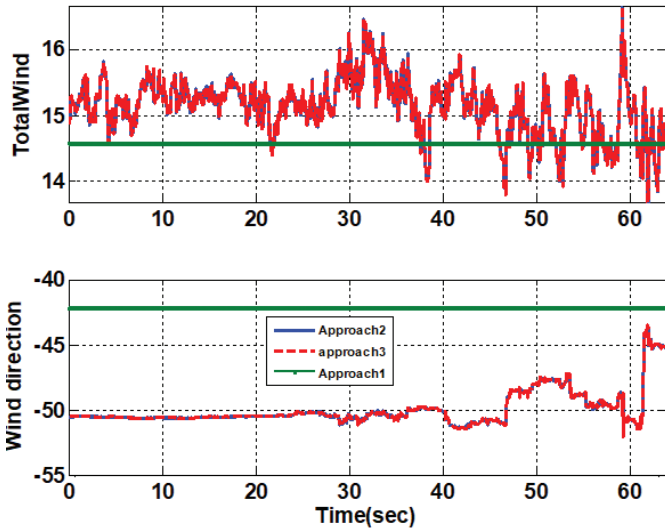**Figure 4. Estimated wind components from roller coaster maneuver.**

Figure 5. Total wind velocity and wind direction for roller coaster maneuver.
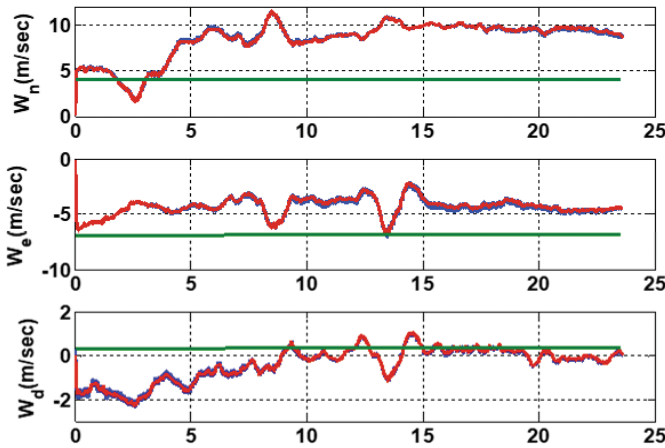

Figure 6. Estimated wind components from Pitch Doublet maneuver in wind up turn.

In Figs. 4 and 6, the estimated wind components from Approach 1 show no change over the duration of data segments, as these are treated as constant biases. In contrast, wind components obtained from Approach 2 and 3 show randomly changing wind velocities which are significantly different from the constant wind velocity values estimated using Approach 1. Further, it is interesting to note that, despite the formulation for wind estimation being very different in Approach 2 and 3, the wind velocities from these two approaches are exceptionally well matched.

Table 1. Estimated biases in accelerations and rates

Parameter	Estimated value	Standard deviation
Δa_x	1.63370e-02	2.1491e-03
Δa_y	-5.17674e-02	2.1287e-02
Δa_z	3.80374e-03	1.2461e-02
Δp	-4.70081e-03	3.1776e-06
Δq	-1.24640e-03	1.2357e-06
Δr	1.51588e-03	4.8576e-06

Figure 7 gives the illustration of what happens if the wind components are not estimated in the process of FPR. The results show the response match between the measured and estimated airspeed and AOA for the full flight data. Wind estimation is omitted in Approach 1 for FPR while Approach 2 and 3 consider wind estimation. Results from Approach 1 show the error in velocity to be around 40m/s while the error in alpha is around 5 deg.

It was observed in Figs. 4 and 6 for the short duration manoeuvres that estimated wind velocities from both the Approaches 2 and 3 are well matched. This is ascertained for the entire duration of the flight of a typical sortie in Fig. 8 where, once again, wind estimation from both the Approaches shows no noticeable deviations (deviation within ±1m/s). Figure 9 shows the total wind variation with time and altitude. It is also seen that between 10 km to 14 km, (stratosphere) the wind shows a definite pattern with altitude[15,21].

Looking at the above results, one may conclude that, compared to Approach 3, wind estimation using Approach 2 could provide for a better option given its computational simplicity. However, it needs to be kept in mind that Approach 2 necessarily requires measurements of inertial velocities and
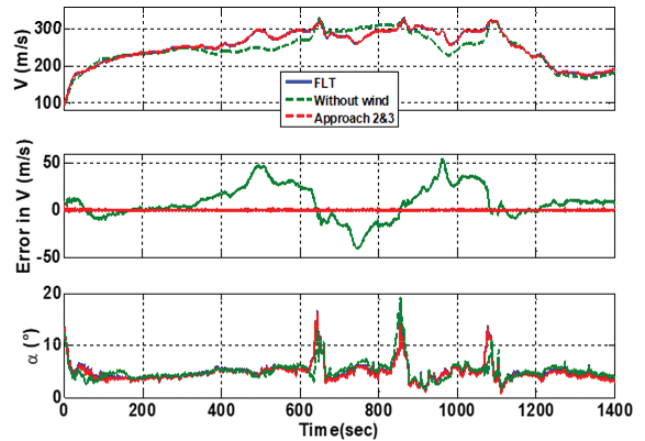

Figure 7. Velocity and flow angles with and without estimating wind (full flight).
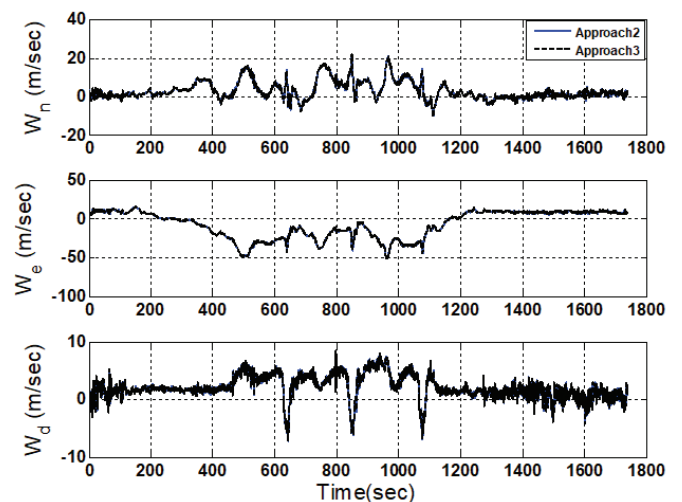

Figure 8. Estimated wind components from Approach 2 and 3 (Full flight).

flow angles for its implementation whereas Approach 3 may still yield reliable estimates in the absence of inertial velocity measurements with proper tuning of process noise covariance matrix.

4.2 Reconstructed Flow Angles

Wind velocities obtained from FPR were illustrated in Figs 4 and 6 for the roller coaster and pitch doublet manoeuvre in windup turn. In the following discussion, we see how this affects the accuracy of the reconstructed α from FPR. In Fig. 10, the reconstructed α from roller coaster data is compared to the reference α obtained from Air Data Computer (ADC). In the α range of upto 16 deg covered during this manoeuvre, all the wind formulations are seen to provide a reasonably good match between the reconstructed and reference α. An error of around 2 deg is observed in α when no winds are estimated in FPR.

Figure 11 shows a similar comparison for the pitch doublet in windup turn. Once again, the reconstructed and reference

α are in good agreement upto 16 deg α. However, the error increases at higher angles-of-attack. The time varying wind formulations used in Approaches 2 and 3 are seen to provide the best match to reference α. Maximum error is seen when no winds are considered. This is also evident from Fig. 12 which shows the enlarged view at higher angles of attack.

The flight manoeuvres considered in Figs. 10 and 11 will not have much excursions in β. However, wind estimation also affects the reconstruction of β during FPR. Figure 13 shows the results from FPR for a rudder doublet manoeuvre. A close match is observed between the reference β response and the reconstructed values obtained using Approaches 2 and 3. In contrast, the constant wind formulation of Approach 1 fails to provide the desired accuracy in β.

To further test the adequacy of Approaches 2 and 3, FPR is carried out for the full flight data from take-off to landing. Figure 14 gives the results of FPR match in the attitudes and Fig. 15 gives the response match for V, α and β. An excellent match is observed between the measured and estimated flight variables that is valid for the entire flight duration.
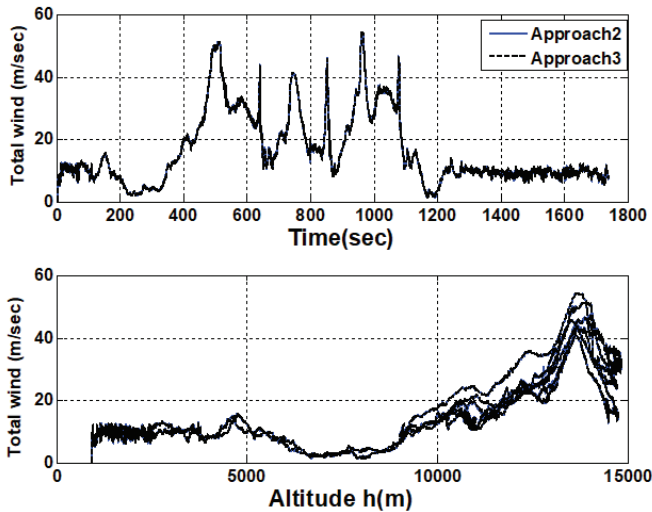

Figure 9.   Total wind variation obtained using Approach 2 and 3 (full flight).
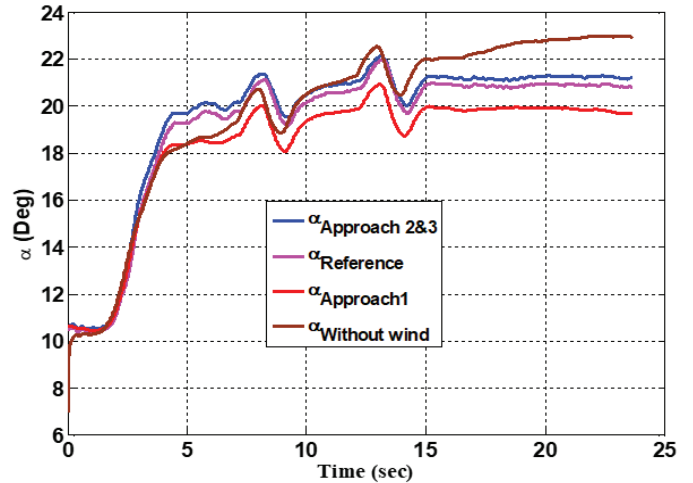

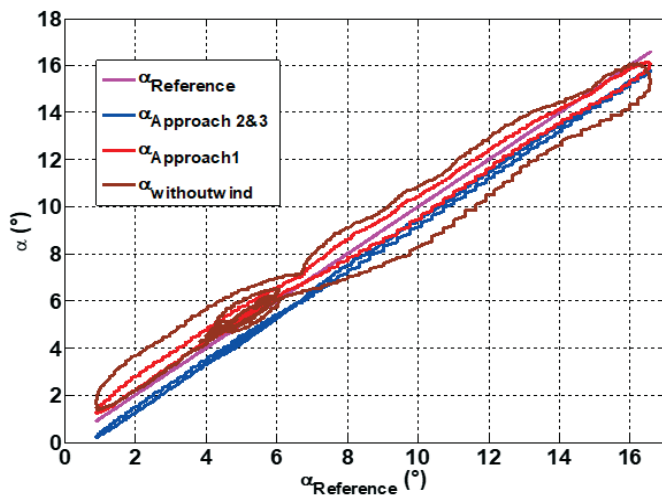Figure 11. Reconstructed α for pitch doublet in windup turn with different wind formulations.

Figure 10. Reconstructed α vs reference α for roller coaster maneuver.

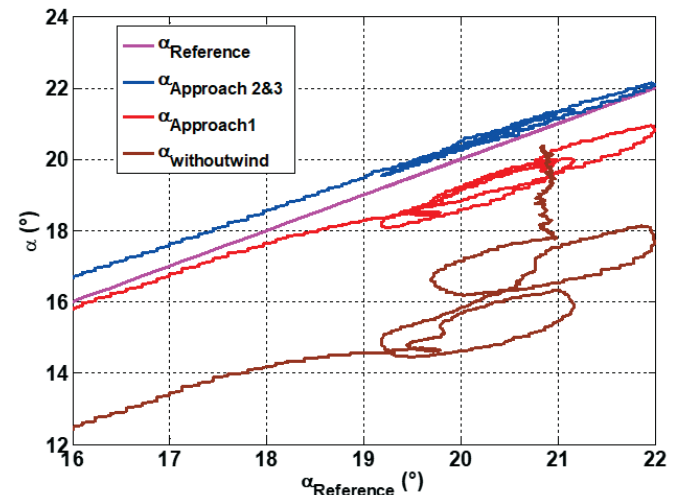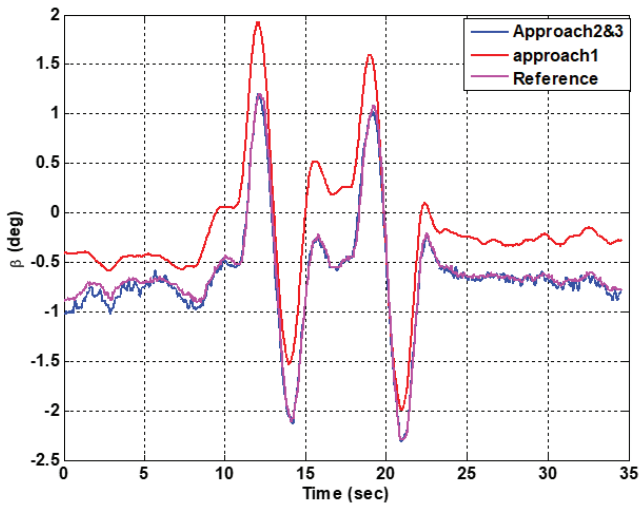Figure 12. Enlarged α comparison for pitch doublet in windup turn.

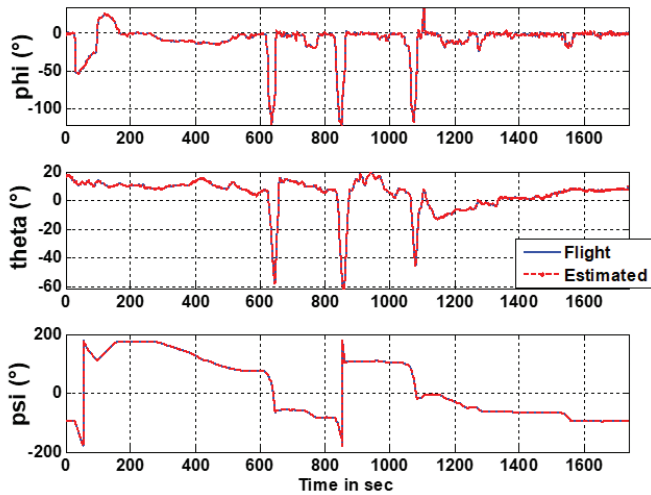**Figure 13. Reconstructed β from FPR of rudder doublet maneuver at high AoA.**

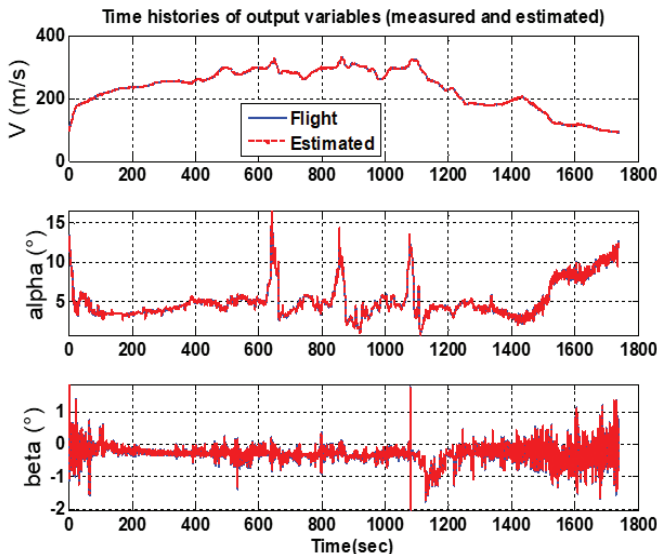

Figure 14. Response match for attitude angles.

Figure 15. Estimated velocity, α and β.

5. CONCLUSIONS

The study brings out the merits and demerits of the different approaches proposed for wind estimation along with aircraft state estimation. The algorithms investigated have the benefit of predicting wind velocities with high accuracy throughout the aircraft sortie, resulting in improved accuracy of the flight trajectories of air data parameters. Time varying wind formulations are seen to give better estimates of flow angles, especially at high angle of attack. Results from the analytical wind model match closely with the state augmented model, when implemented as part of state estimation using EKF. The variation of wind profile with altitude is also well captured with the proposed algorithms.

REFERENCES

1. Jategaonkar, R.V. Flight vehicle system identification: A time domain methodology. AIAA, Reston, VA, 2006.
2. Haering, E. A. Air data calibration of a high-performance aircraft for measuring atmospheric wind profiles. NASA TM-101714, 1990.
3. Chowdhary, Girish & Jategaonkar, Ravindra. Aerodynamic parameter estimation from flight data applying extended and unscented Kalman filter. *Aerospace Sci. Technol.,* 2010, **14**(2), 106–117.
4. Nusrath, K.; Sarmah, A. & Singh, J. Flight path reconstruction and wind estimation using flight test data from crash data recorder (CDR). *SAE Technical Paper*, 2014, 2014-01-2168.
   doi:10.4271/2014-01-2168
5. Jared, A. Grauer. Real-time data-compatibility analysis using output-error parameter estimation. 2015, **52**(3), 940-947,
   doi:10.2514/1.C033182
6. Teixeira, Soares; Torres, Leonardo; Henriques, Paulo; Oliveira, Iscold & Aguirre, Luis. Flight path reconstruction using the unscented Kalman filter algorithm. *In* 18th International Congress of Mechanical Engineering, Ouro Preto, MG, Nov. 6-11, 2005.
7. Parks, E.K.; Wingrove, R.C.; Bach, R.E. Jr. & Mehta, R.S. Identification of vortex-induced clear-air turbulence using airline flight records. *Journal Aircraft,* 1985, **22**(2), 124-129.
8. Lewis, G. Using GPS to determine pitot-static errors. National Test Pilot School, Mojave, California, 2003.
9. Meir, Pachter.; Nicola, Ceccarelli & Phillip, R. Chandler. Estimating MAV's heading and the wind speed and direction using GPS, inertial, and air speed measurements. *In* Proceedings of AIAA Guidance, Navigation & Control conference and exhibit, Hawaii, 2008-6311.
   doi:10.2514/6.2008-6311
10. Mulgund, Sandeep S. & Robert, F. Stengels. Optimal nonlinear estimation for aircraft flight control in wind shear. *Automatica*, 1996, **32**(1), 3-13.
11. Gratton, G. B. Use of Global Positioning system velocity outputs for determining airspeed measurement error. *The Aeronautical Journal*, 2007, **111**(1120), 381-388.
12. Bach, R.E. & Wingrove, R.C. Analysis of wind shear from airline flight data. *AIAA Journal Aircraft*, 1989, **26**(2),

103-109.

13. Bach, R.E. Jr. & Parks, E.K. Angle-of-Attack estimation for analysis of windshear encounters. *AIAA Journal Aircraft,* 1987, **24**(11), 789-792.

14. Brian, R. Taylor. A Full-Envelope Air data calibration and three-dimensional wind estimation method using global output-error optimization and flight-test techniques. *In* AIAA Conference, August 2012.
doi:10.2514/6.2012-4410

15. De Jong, P. M. A.; van der Laan, J. J.; int Veld, A.C.; van Paassen, M. M. & Mulder, M. Wind-profile estimation using airborne sensors. *AIAA Journal Aircraft,* 2014, **51**(6).
doi:10.2514/1.C032550

16. Cho, A.M.; Jihoon, Kim; Sanghyo, Lee & Changdon, Kee. Wind estimation and airspeed calibration using a UAV with a single-antenna gps receiver and pitot tube. *IEEE Trans. Aerospace Electron. Syst.,* 2011, **47**(1), 109-117.
doi:10.1109/ TAES. 2011. 5705663

17. Lee, Je Hyeon; Hakki, Erhan Sevil; Atilla, Dogan & David, Hullender. Estimation of maneuvering aircraft states and time varying wind with turbulence. *Aerospace Sci. Technol.*, 2013, **31**(1), 87–98.

18. Madapusi, H.J. Palanthandalam; Girard, A. & Bernstein, D.S. Wind field recon-struction using flight data. *In* Proceedings of the American Control Conference, Seattle, WA, 2008, 1863–1868.
doi:10.1109 /ACC.2008.4586763

19. Kamali, C. & Erol, Ozger. Limitations of flight path reconstruction techniques, *Sadhana,* 2019, **44**(2), 1-15.
doi:10.1007/s12046-018-1019-3

20. Wingrove, R.C. & Bach, R.E. Severe winds in the DFW microburst measured from two aircraft. *J. Aircraft*, 1989, **26**(3), 221-224.
doi:10.2514/3.45749

21. Ching Yaw Tzeng. Wind shear estimation along the trajectory of an aircraft. Rice University, Texas, 1989. (PhD Thesis).

ACKNOWLEDGMENT

CONTRIBUTORS

Ms Khadeeja Nusrath T.K. holds BTech (Instrumentation & Control) from the University of Calicut and MTech (Electronics) from Visvesvaraya Technological University. Currently working as a Principal scientist at the Flight Mechanics and Control Division of CSIR-NAL Bengaluru. She has been extensively involved in aircraft/rotorcraft system identification and parameter estimation. She has several research papers to her credit.
In the current study, she has developed the algorithms for flight path reconstruction and wind estimation and also carried out the data analysis.

Dr Jatinder Singh receieved his PhD in Aerospace Engineering from IIT Kanpur and a recipient of the Alexander von Humboldt Fellowship. Presently working as Chief scientist & Head of Flight Mechanics and Control Division of CSIR-NAL. He has been extensively involved in aircraft modeling and parameter estimation work and has several conference and journal papers to his credit. He has also co-authored two books.
In the current study, he has provided the ideas and guidance which has led to the work presented in this paper.